THE JOURNAL OF BIOLOGICAL CHEMISTRY VOL. 289, NO. 22, pp. 15845–15855, May 30, 2014

Structural and Functional Profiling of the Lateral Gate of the Sec61 Translocon*

Received for publication, November 12, 2013, and in revised form, April 17, 2014 Published, JBC Papers in Press, April 21, 2014, DOI 10.1074/jbc.M113.533794

Johannes H. Reithinger[‡], Chewon Yim[§], Sungmin Kim[§], Hunsang Lee[§], and Hyun Kim[§1]

From the [§]School of Biological Sciences, Seoul National University, Seoul 151-747, South Korea and [‡]Center for Biomembrane Research, Department of Biochemistry and Biophysics, Stockholm University, SE-106 91 Stockholm, Sweden

Background: The Sec61 lateral gate mediates transmembrane segment insertion into the ER membrane.
Results: Interactions and the effects of mutations of the Sec61 lateral gating helix residues were determined.
Conclusion: Key residues that modulate translocation, membrane insertion, and topogenesis of membrane proteins are identified.
Significance: This study offers mechanistic and structural insights into Sec61 gating.

The evolutionarily conserved Sec61 translocon mediates the translocation and membrane insertion of proteins. For the integration of proteins into the membrane, the Sec61 translocon opens laterally to the lipid bilayer. Previous studies suggest that the lateral opening of the channel is mediated by the helices TM2b and TM7 of a pore-forming subunit of the Sec61 translocon. To map key residues in TM2b and TM7 in yeast Sec61 that modulate lateral gating activity, we performed alanine scanning and *in vivo* site-directed photocross-linking experiments. Alanine scanning identified two groups of critical residues in the lateral gate, one group that leads to defects in the translocation and membrane insertion of proteins and the other group that causes faster translocation and facilitates membrane insertion. Photocross-linking data show that the former group of residues is located at the interface of the lateral gate. Furthermore, different degrees of defects for the membrane insertion of single- and double-spanning membrane proteins were observed depending on whether the mutations were located in TM2b or TM7. These results demonstrate subtle differences in the molecular mechanism of the signal sequence binding/opening of the lateral gate and membrane insertion of a succeeding transmembrane segment in a polytopic membrane protein.

The evolutionarily conserved SecY/61 (SECretory Y/61) complex forms a channel in the membrane of the endoplasmic reticulum (ER)[2] and mediates translocation and membrane insertion of proteins. This complex is a heterotrimer comprising Sec61α (Sec61p/SecY), Sec61β (Sbh1p/SecE), and Sec61γ (Sss1p/SecG) in mammals (yeast/prokaryotes). Protein translocation and insertion occur either co- or post-translationally (1). In the co-translational mode, the signal sequence is recognized by the signal recognition particle (SRP), and the SRP-ribosome-nascent chain complex is targeted to the translocon (2). For post-translational translocation, the Sec62-Sec63 complex assembles with the Sec61 translocon (3, 4).

The x-ray structure of the archaeal-bacterial SecY complex revealed that SecY subunit is divided into two bundles of five transmembrane (TM) helices (TM1–5 and TM6–10), forming an hourglass-shaped pore with the loop between TM5 and TM6 serving as a hinge (5–7). The extracytoplasmic funnel of the pore is sealed by a short helical plug domain (TM2a). The narrow constriction in the middle of the channel, called the pore ring, consists of conserved hydrophobic residues. Together, the pore ring and plug seal the channel, preventing the flow of ions and metabolites across the membrane (8). Structural and cross-linking data suggest that TM2b and TM7, which are located opposite to the hinge, presumably form the lateral gate that allows TM segments of nascent chains to exit into the lipid bilayer and serve as the signal sequence binding site during the early stages of translocation (5–7, 9–12).

To allow protein translocation and/or integration into the lipid bilayer, the translocon has to undergo conformational changes; that is, displacement of the plug and opening of the lateral gate. The SecY structures bound to SecA or a ribosome allow the first glimpse of the semi-open state of the lateral gate (6, 7, 13). The plug was shown to be important for efficient protein translocation, the orientation of signal anchor proteins, and Sec61 complex stability (14, 15). Mutations that allow the translocation of proteins with defective signal sequences in *Escherichia coli* (*prl* mutations) (16–18) are predominantly found in the plug domain, the pore ring, and the lateral gate forming TM2b and TM7 (5, 19, 20). Recent findings show that conserved residues in the pore ring and the lateral gate define the hydrophobicity threshold for signal sequence insertion and membrane integration (11, 21, 22). Furthermore, a hydrogen-bond cluster between TM2, TM3, and TM7, which connects the two sides of the gate, has been proposed to play an important role in regulating the open and closed conformations of the Sec61 translocon (22, 23).

Systematic measurements of potential TM segment integration (24–27) and molecular dynamics simulations (28–30) suggest that the process for the initial TM segment insertion from the translocon to the membrane is a thermodynamic event in

* This work was supported by Basic Research Grant 2013R1A1A2A10010894 and Global Research Network Grant 202-2001-1-C00031 from the National Research Foundation of Korea (to H. K.).
[1] To whom correspondence should be addressed: School of Biological Sciences, Bldg. 504-421, Seoul National University, Seoul 151-747, South Korea. Tel.: 82-2-880-4440; Fax: 82-2-872-1993; E-mail: joy@snu.ac.kr.
[2] The abbreviations used are: ER, endoplasmic reticulum; Bpa, benzo-L-phenylalanine; IP, immunoprecipitation; Lep, leader peptidase; TM, transmembrane; 2G, double-glycosylated; 1G, single-glycosylated.

which Sec61 provides a conduit through which polypeptide chains can partition into or translocate across the membrane (10). However, it is unclear whether partitioning is only passively facilitated by a "breathing" translocon (31), which continuously opens and closes toward the lipid bilayer or whether signal sequence/TM segment binding triggers an active response from the translocon and influences the kinetics of signal sequence binding and TM segment insertion. In cases of membrane insertion of multispanning membrane proteins, cross-linking and fluorescence studies have shown that associations between the TM domain(s) and the translocon and the timing of their release into the lipid bilayer vary depending on sequence context, suggesting that the Sec61 complex may play an active role in TM helix insertion (32–35). A recent study by Cymer and von Heijne (36) shows that interaction between TM helices could occur co-translationally at the exit site of the Sec translocon.

Despite an abundance of data, the molecular mechanism by which the lateral gate of the Sec61 translocon functions remains elusive. We took two approaches to determine key residues that modulate lateral gating activity: systematic alanine scanning and *in vivo* site-directed photocross-linking of the TM2b and TM7 of the *Saccharomyces cerevisiae* Sec61. These approaches identified key residues modulating membrane insertion efficiency of a marginally hydrophobic TM segment and created an interaction profile between TM2b and TM7 of the yeast Sec61.

EXPERIMENTAL PROCEDURES

Plasmids and Strains—pDQ1-WT (Leu) contains the wild type (WT) *SEC61* gene, including its endogenous promoter (37, 38). For alanine scanning, Ala codons were introduced in *SEC61* one at a time by site-directed mutagenesis using pDQ1-WT as a template. The sequences were verified by DNA sequencing. pDQ1-WT and the generated mutants were transformed into the Δ*sec61* strain RSY1293 pH-Sec61-YCplac33 (*MATα*, *ura3-1*, *leu2-3,112*, *his3-11,15*, *trp1-1*, *ade2-1*, *can1-100*, *sec61*::*HIS3* [pH6-Sec61-YCplac33]) (37, 38). pH6-Sec61-YCplac33 (Ura) contains the WT *SEC61* gene. Functional complementation of Sec61 variants was assessed by plating the mutant strains on 5-fluoroorotic acid-containing −Leu SD plates, which were grown for 3 days at 30 °C. For complete removal of pH-Sec61-YCplac33, streaking on 5-fluoroorotic acid plates was repeated three times. To assess the influence of Ssh1 on model protein translocation, pDQ1-WT and selected plasmids with *sec61* variants were transformed into the Δ*sec61*Δ*ssh1* double deletion strain, RSY1293 (Δ*ssh1*) pH-Sec61-YCplac33 (*MATα*, *ura3-1*, *leu2-3112*, *his3-11,15*, *trp1-1*, *ade2-1*, *can1-100*, *sec61*::*HIS3*, *ssh1*::*TRP1* [pH6-Sec61-YCplac33]) (37).

Amber stop codons and Factor Xa cleavage sites for photocross-linking experiments were also introduced into pDQ1-WT via site-directed mutagenesis. Factor Xa cleavage site was introduced into the loops 1, 2, 5, 6, or 7 at positions after Ser-57, Ser-107, Arg-207, Ile-269, or Ser-351, respectively. Residues in TM2b and TM7 were replaced with an amber codon one at a time in the background of pDQ1 plasmids containing Factor Xa cleavage sites of varying positions. The amber mutation and Factor Xa cleavage site carrying pDQ1 plasmids and the plasmid encoding amber suppressor tRNA synthetase and its cognate tRNA were co-transformed into W303–1α cells (*MATα*, *ade2*, *can1*, *his3*, *leu2*, *trp1*, *ura3*).

Proteasome Inhibition—Proteasome inhibition using MG132 was carried out as described in Liu *et al.* (39). RSY1293 (Δ*ssh1*) cells expressing either Sec61 WT or I91A were transformed with plasmids encoding Lep-H1(5L/14A) model protein. The yeast cells were grown overnight at 30 °C in a synthetic medium containing L-proline as the sole nitrogen source with appropriate amino acids. The culture was re-inoculated in the same medium with 0.003% SDS at A_{600} of 0.5 and grown for 3 h at 30 °C until A_{600} reached ~1.0. For pulse-chase experiment, 9 A_{600} units of cells were harvested for each reaction and incubated in a proline-based medium lacking methionine supplemented with either MG132 (100 μM) or the control buffer with dimethyl sulfoxide (DMSO) for 30 min at 30 °C. Cells were subjected to pulse-chase experiments after incubation, and MG132 concentration was kept at 100 μM during the whole chase time.

Photocross-linking—The W303–1α (*MATα*, *ade2*, *can1*, *his3*, *leu2*, *trp1*, *ura3*) was transformed with two plasmids, one carrying Sec61 with an amber mutation and the other carrying the amber suppressor tRNA-synthetase and its cognate tRNA (40). The yeast cells were grown at 30 °C on −Leu −Trp medium to an optical density at 600 nm (A_{600}) of 1.0. Exponentially growing cultures were then diluted to A_{600} = 0.2, supplemented with 1 mM benzo-L-phenylalanine (Bpa) in 1 mM NaOH, and grown to an A_{600} of 0.5. Cells were harvested by centrifugation at 3200 rpm. Cell pellets were resuspended in 1 ml of −Leu −Trp medium, and half of the cell pellets were mixed with an additional 2.5 ml of medium, transferred to a Petri dish (60 × 15 mm) on ice, and then irradiated with ultraviolet (UV) radiation at 365 nm for 30 min. The other half of the cell pellets was kept on ice.

After cell lysis with glass beads, immunoprecipitation (IP) was performed by heating the cross-linked samples for 10 min at 55 °C in the presence of 1% SDS followed by centrifugation at 16,000 × *g* for 10 min. Four volumes of immunoprecipitation buffer (10 mM Tris-HCl, pH 7.6, 140 mM NaCl, 1 mM EDTA, 1% Triton X-100) were then added to the aliquots of the resulting supernatant. The mixture was incubated with gentle rotation in the presence of protein G-agarose, which was prewashed twice with IP buffer, and anti-HA antiserum (Covance) for 3 h at room temperature. The IP product was washed twice with IP buffer and once with Buffer C (10 mM Tris-HCl, pH 7.5, 50 mM sodium chloride).

Factor Xa Digestion—The IP products were treated with 1 μl of Factor Xa (New England Biolabs, Ipswich, MA) for 2 h at 23 °C in 100 μl of Xa buffer (20 mM Tris-HCl, pH 8.0, 100 mM sodium chloride, 2 mM calcium chloride), which was adjusted to 0.017% SDS. After Factor Xa treatment, the same washing steps used for immunoprecipitation were performed followed by incubation with SDS-PAGE sample buffer at 55 °C for 10 min before running on SDS gel.

Pulse-labeling, Pulse-chase, and IP—Cell labeling, pulse-chase, lysis, and IP were performed as previously described (41). Immunoprecipitated proteins were subjected to SDS-PAGE

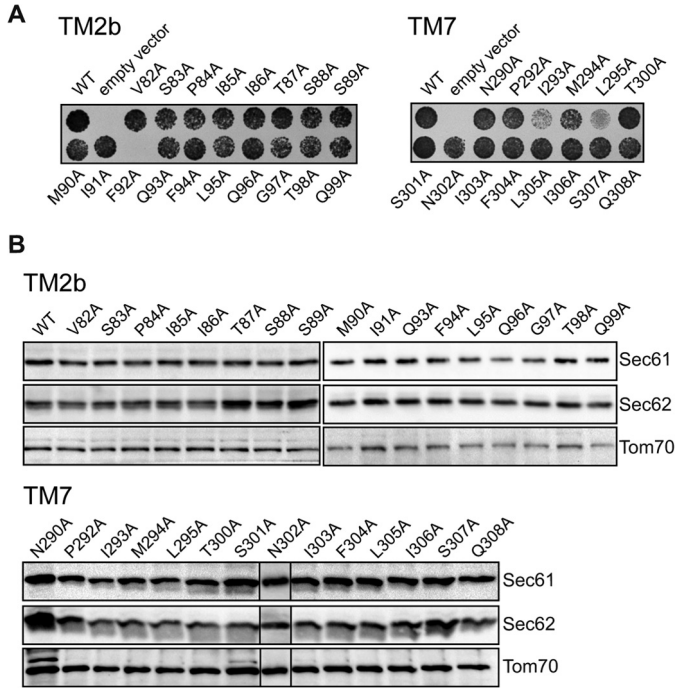

FIGURE 1. **Alanine scanning of TM2b and TM7 of Sec61 had little or no effect on translocon functionality and stability.** *A*, complementation assay in yeast cells expressing WT or mutant Sec61 by plasmid shuffling. Δ*sec61* cells carrying the Ura-born WT *SEC61* were transformed with WT or *sec61* variants in Leu-born plasmids. Cells were grown on −Leu plates containing 5-fluoroorotic acid and incubated for 3 days at 30 °C. *B*, relative expression levels of Sec61 with single Ala substitutions in TM2b or TM7, and Sec62 were assessed by Western blotting. Tom70, a mitochondrial outer membrane protein served as a loading control.

and quantified using Fuji FLA-3000 phosphorimaging and the Image Reader V1.8J/Image Gauge V 3.45 software.

Western Blot Analysis—Yeast protein analysis by Western blotting was performed as previously described (41). Anti-HA antiserum (Covance) was used for detection of the model substrates.

RESULTS

Alanine Scanning of TM2b and TM7 of Sec61—To probe which residues in TM2b and TM7 of Sec61 are critical for the lateral gating function, systematic mutagenesis of these helices was performed. Residues 82–99 in TM2b and 290–308 in TM7 were substituted with an Ala residue one at a time. Functional complementation by Sec61 variants was assessed by plasmid shuffling in a *sec61* deletion strain carrying the WT *SEC61* on a Ura-born plasmid. With the exception of F92A, all the mutants were viable, although I293A and L295A showed slower growth, indicating that these Sec61 mutants could functionally replace the WT protein (Fig. 1*A*). Sec61 has been shown rather insensitive to mutations (15, 17, 21, 22, 37). In case these Sec61 mutants disrupt the complex formation, thereby impairing the stability of individual subunits, we assessed the relative expression levels of the Sec61 mutants and Sec62 by Western blotting analysis (Fig. 1*B*). The protein expression levels of the Sec61 variants and Sec62 are comparable with the WT. This result indirectly indicates that the stability of the Sec61 mutants or Sec62 is not compromised.

Identifying Sec61 Mutants That Increase or Decrease the Translocation and Membrane Insertion Efficiency of a Single-spanning Membrane Protein—Each Sec61 Ala mutant strain was transformed with a set of model protein constructs to assess how each Sec61 mutant handles the targeting and membrane insertion of model proteins of varying sequence context. First, we determined the efficiency of targeting and membrane insertion for a model single-spanning membrane protein derived from *E. coli* leader peptidase (Lep) (27). In this protein the original two N-terminal TM segments were replaced with a hydrophobic segment (H1-segment) consisting of 5 Leu and 14 Ala residues (Fig. 2*A*). We selected H1-segment with threshold hydrophobicity (5L/14A) because this segment enables sensitive detection of the insertion efficiencies of Sec61 gate mutants. The H1-segment can act as a signal sequence that targets the protein to the ER and as a TM domain (27, 41). Interestingly, this model protein, Lep-H1, is integrated into the membrane with dual membrane topology (N_{out}-C_{in} (*left*) and N_{in}-C_{out} (*right*) membrane orientations; Fig. 2*A*). Lep-H1 contains one glycosylation site at the N terminus and two at the C terminus; thus, both membrane targeting and integration with either N_{in}-C_{out} or N_{out}-C_{in} topology can be monitored by assessing the glycosylation status: a double-glycosylated form (2G) indicates membrane insertion in the N_{in}-C_{out} orientation, a single-glycosylated form (1G) indicates membrane insertion in the N_{out}-C_{in} orientation, and an unglycosylated form (0G) indicates a non-translocated/non-targeted protein (Fig. 2*B*). For rare cases, we observed a triple-glycosylated form (3G) that represents a fully translocated protein.

A plasmid encoding Lep-H1(5L/14A) was transformed into the Sec61 mutant strains, and each transformant was subjected to 5 min of [S^{35}]Met radiolabeling and subsequent IP and analyzed by autoradiography. The Lep-H1(5L/14A) segment is moderately hydrophobic (ΔG of membrane insertion = −1 kcal/mol) and has ~48% targeting efficiency (glycosylated products/total products) in WT Sec61 (Fig. 2*B*). Compared with WT, the targeting efficiency of the model protein was increased by ~10% for the V82A, I86A, Q96A, I293A, F304A, and S307A Sec61 mutants (Fig. 2*C*). Interestingly, in these mutants the model protein that was integrated into the membrane with an N_{in}-C_{out} orientation was enhanced (45–54% in the mutants compared with 33% in WT) (Fig. 2*D*).

We identified the second group of Sec61 mutants that decreased the insertion of the Lep-H1 model protein. In Sec61 mutants S83A, M90A, I91A, Q93A, F94A, L95A, N290A, P292A, L295A, and N302A, ~20% less of the Lep-H1 model protein was integrated into the membrane compared with WT (Fig. 2*C*). These mutations also decreased the relative amount of Lep-H1 with an N_{in}-C_{out} membrane topology (Fig. 2*D*).

Dissecting Mechanisms for the Increased or Decreased Efficiency of Translocation and Membrane Insertion in Sec61 Mutants—To determine whether the increase or decrease in Lep-H1(5L/14A) translocation in Sec61 mutants during 5 min of pulse-labeling would eventually reach the WT level, we performed pulse-chase experiments. WT, V82A, I86A, I91A, and N302A Sec61 mutant strains containing Lep-H1(5L/14A) were subjected to pulse-chase and IP and analyzed by autoradiography (Fig. 3*A*). The V82A and I86A Sec61 mutants had faster

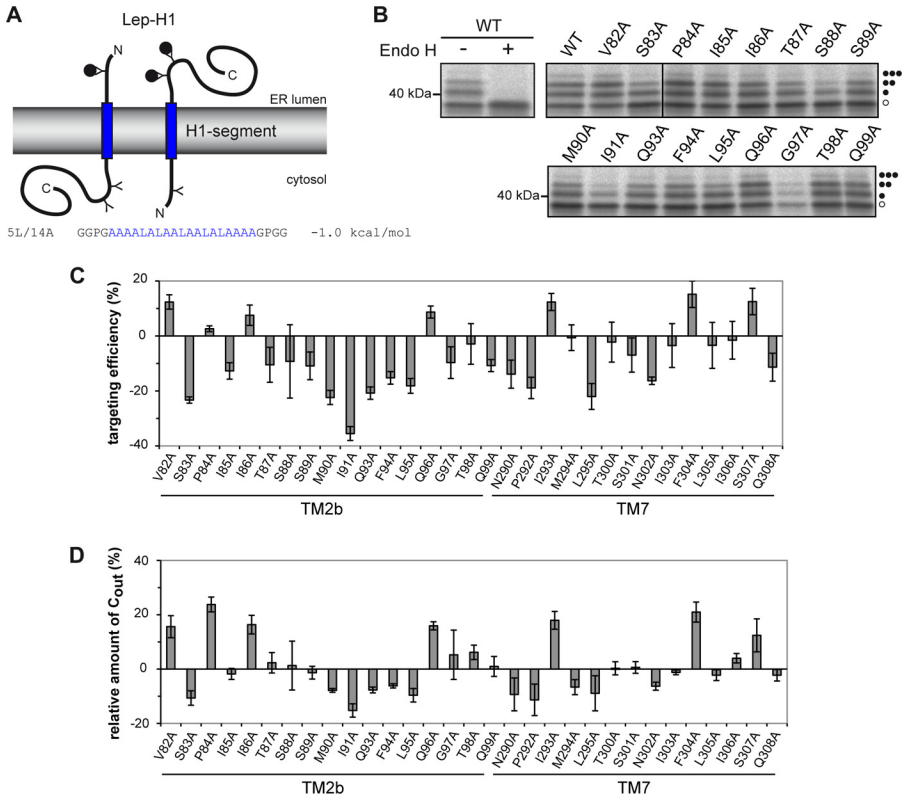

FIGURE 2. **The targeting and membrane insertion of a single-spanning membrane protein in Sec61-gating helix mutants.** *A*, the Lep-H1(5L/14A) model protein. The H1-segment sequence with its apparent free energy of insertion (Δ*G*) is indicated. *B*, WT cells expressing the model protein were radiolabeled with [^{35}S]Met for 5 min and subjected to IP and SDS-PAGE and analyzed by autoradiography. Before SDS-PAGE, one sample was split into two samples, one of which was treated with endoglycosidase H (*Endo H*) to remove all glycans. Different glycosylation states are indicated with *closed circles*. *Open circle* indicates an unglycosylated form. *C*, the deviations of the Lep-H1(5L/14A) membrane targeting efficiencies of the Sec61 mutant strains normalized to the WT level are plotted. The targeting efficiencies were calculated as the amount of glycosylated products over the total products. The average plus S.E. for at least three independent measurements is shown. *D*, the relative amount (%) of Lep-H1(5L/14A) with an N_{in}-C_{out} membrane topology was calculated as 2G/(1G + 2G) × 100% using the same data set in *B* and normalized against the WT level.

translocation in a 5-min chase, but translocation was not increased further and eventually reached the WT level during a 15-min chase (Fig. 3*A*, *left panel*). In contrast, I91A and N302A exhibited slower translocation, and the translocation efficiency did not reach the WT level in a 15-min chase (Fig. 3*A*, *left panel*).

In the V82A and I86A Sec61 mutants, the relative amount of Lep-H1(5L/14A) protein inserted in the N_{in}-C_{out} orientation was ~2-fold more than that for the WT during a 5-min chase (Fig. 3*A*, *right panel*). Although the protein targeting in the WT eventually reached that of the V82A and I86A Sec61 mutants during a 15-min chase, the ratio of the Lep-H1(5L/14A) protein in the N_{in}-C_{out} orientation remained ~2-fold more for the V82A and I86A Sec61 mutants compared with the WT during a 15-min chase. In the case of the I91A and N302A Sec61 mutants, the relative amount of Lep-H1(5L/14A) protein inserted in the N_{in}-C_{out} orientation was decreased and changed little during a 15-min chase (Fig. 3*A*, *right panel*).

To determine whether unglycosylated proteins are degraded by the proteasome in the cytosol or slowly targeted, we carried out the experiment with the proteasome inhibitor, MG132 (Fig. 3*B*). In the presence of MG132, more unglycosylated protein was detected compared with the sample without MG132, indicating that some of unglycosylated proteins are degraded by the proteasome in the cytosol (~10% for both Sec61 WT and I91A mutant), but the glycosylated products were still increased over the chase time, suggesting that some unglycosylated proteins are slowly translocated/membrane-inserted.

These data suggest that the V82A and I86A Sec61 mutants are pre-opened or have faster channel opening, whereas I91A and N302A Sec61 mutants are more prone to remain in a closed conformation or slowly open. These results further imply that the orientation of a TM domain is influenced by the status of the Sec61 channel opening when the TM domain enters into the pore.

Ssh1 Has Little Effects on the Membrane Insertion of Model Proteins in Sec61 Mutant Strains—Ssh1, a homolog of Sec61 in yeast, mediates protein translocation, but cells are viable upon its deletion (42, 43). To determine whether Ssh1 influences the membrane insertion efficiency and orientation of a model protein in the Sec61 mutant background, we tested the Lep-H1(5L/14A) protein in the absence of Ssh1 using an *ssh1* deletion strain. Although targeting efficiency was reduced by ~3–17% in the absence of Ssh1, the pattern of effects due to the Sec61 mutations remained the same (Fig. 4*A*). Furthermore, membrane insertion in the N_{in}-C_{out} orientation was unchanged regardless of the presence or the absence of Ssh1 (Fig. 4*B*). These results suggest that Ssh1 has little influence on the observed effects of the targeting and membrane insertion of model proteins in the Sec61 mutant strains.

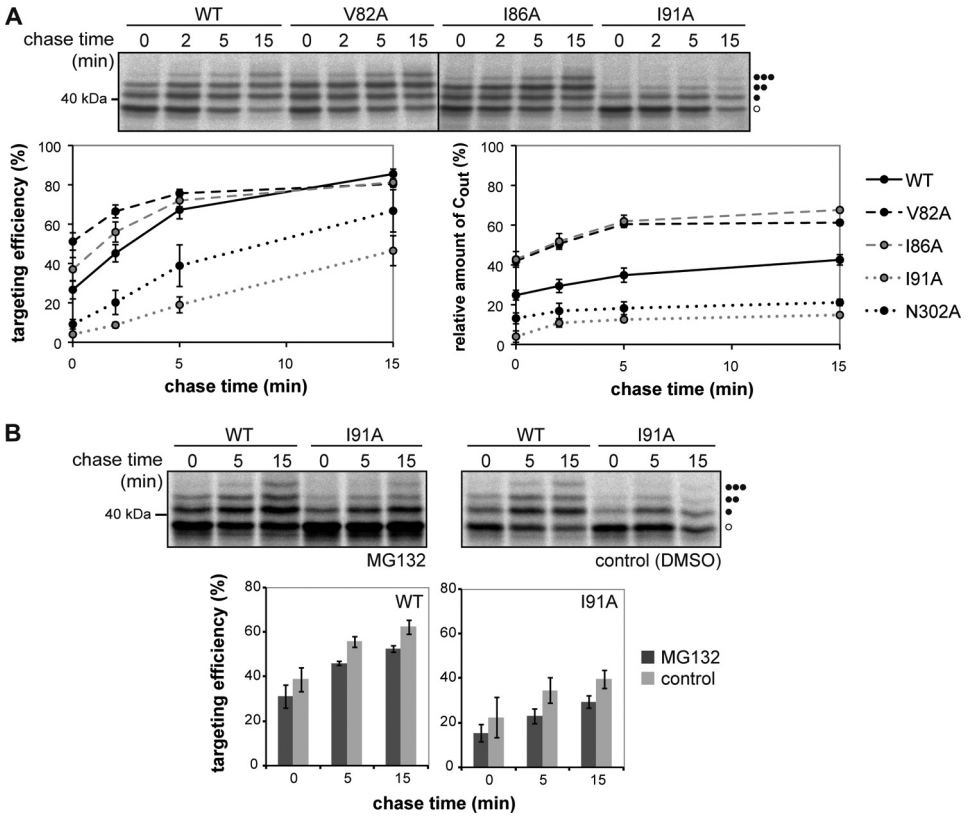

FIGURE 3. **Different kinetics of Sec61-gating helix mutants.** *A*, the Lep-H1(5L/14A) model protein was labeled with [^{35}S]Met in the Sec61 WT and mutant strains (V82A, I86A, I91A, N302A) for 5 min and chased for 0, 2, 5, and 15 min with cold Met. Samples were subjected to IP with an anti-HA antibody and SDS-PAGE and analyzed by autoradiography. The amount of glycosylated products was quantified and plotted as the targeted Lep-H1(5L/14A) model protein (%) against the chase time for the WT, V82A, I86A, I91A, and N302A strains (*left*). The relative amount of model proteins with N_{in}-C_{out} topology was calculated as 2G/(1G + 2G) × 100% and plotted against the chase time (*right*). The average of three independent measurements plus S.E. is shown. *B*, the Lep-H1(5L/14A) model protein was labeled with [^{35}S]Met in the Sec61 WT and I91A strains for 5 min and chased for 0, 5, and 15 min with cold Met in the presence or the absence of proteasome inhibitor MG132. The amount of glycosylated products is analyzed as described in *A*. The average of three independent measurements plus S.D. is shown.

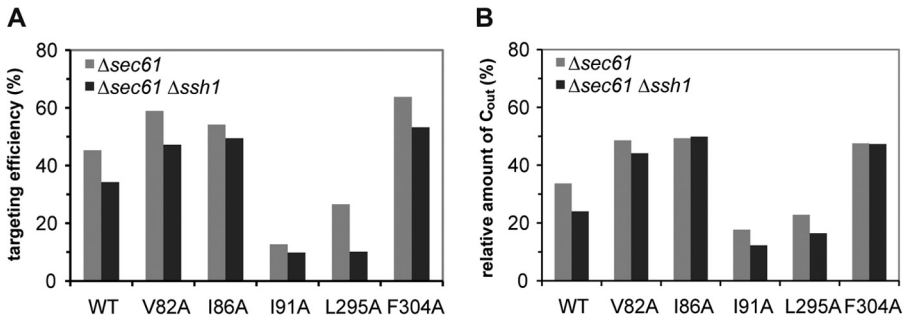

FIGURE 4. **Ssh1 does not significantly influence the effects of the Sec61 mutations on protein translocation and membrane integration.** *A*, to assess whether Ssh1 influences the translocation of Lep-H1(5L/14A), the model protein was expressed in Δ*sec61* Δ*ssh1* cells carrying WT or mutant Sec61. Cells were radiolabeled and treated as described in Fig. 2. Glycosylated products were quantified and plotted as targeting efficiency (%). *B*, the relative amount of Lep-H1(5L/14A) with an N_{in}-C_{out} topology was calculated as 2G/(1G + 2G) × 100%. The average of two independent experiments is shown.

Mutations in TM2b and TM7 Exhibit Different Severity of Defects in the Membrane Insertion of Single- Versus Double-spanning Membrane Proteins—The TM segment in single-spanning membrane proteins initiates translocation, opens the Sec61 lateral gate, and positions itself in the N_{in}-C_{out} or N_{out}-C_{in} orientation before membrane insertion. However, the mechanism of the membrane insertion of the downstream TM domain in multispanning membrane proteins may differ because the initial opening of the channel is not required. To test this, we used the Lep-H2 model protein, the membrane insertion of which was previously analyzed in detail both in mammalian and yeast systems (27). This protein contains two hydrophobic segments with two *N*-linked glycosylation sites, one at the N terminus and the other at the downstream of the second TM segment (Fig. 5*A*, *left panel*). A triple hemagglutinin (HA) tag was fused at the C terminus of the protein to facilitate immunoprecipitation against an anti-HA antibody. The first TM segment is the original first TM segment of *E. coli* Lep and is shown to efficiently target the protein to the ER (27). The second segment was replaced by an engineered segment (H2-segment), consisting of 2L/17A (H2–2L, $\Delta G = 0.7$ kcal/mol) or 3L/16A (H2–3L, $\Delta G = 0.0$ kcal/mol) (Fig. 5*A*, *left panel*). If the

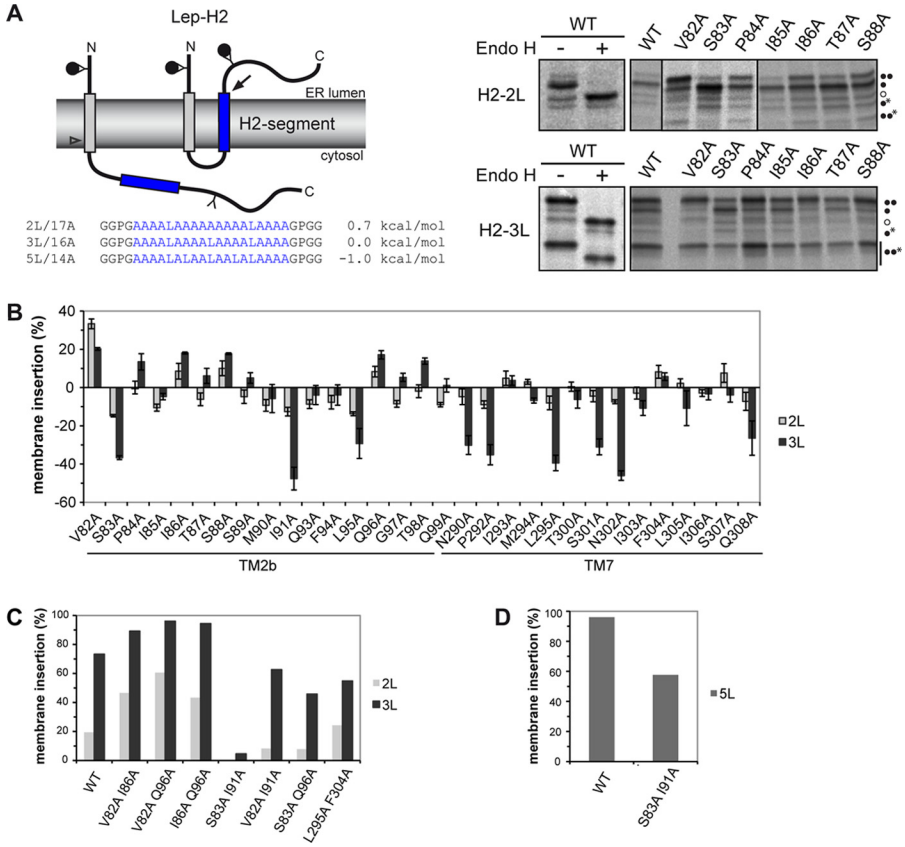

FIGURE 5. **Membrane insertion of the second TM segment of Lep-H2 model proteins in the Sec61 TM2b and TM7 mutants.** *A*, the Lep-H2 model protein has two potential TM domains. The H2-segment is shown as a *blue rectangular box*, and sequences with their apparent free energy of insertion (Δ*G*) are indicated. *N*-Linked glycosylation sites are indicated as *Y*, and occupied sites are shown with *closed circles*. *Open* and *closed arrows* indicate the cleavage sites for cleaved products, 1G* and 2G*, respectively. Cells were radiolabeled for 5 min with [^{35}S]Met, subjected to IP and SDS-PAGE, and analyzed by autoradiography. Endoglycosidase H (*Endo H*) treatment was carried out to remove all glycans before SDS-PAGE. Different glycosylation states are indicated with *closed circles*, including different cleaved products indicated with an *asterisk* (*right*). The *open circle* indicates an unglycosylated full-length protein that is untargeted. *B*, the H2-segment membrane insertion efficiency (%) was calculated as (2G + 2G*)/(1G + 2G + 1G* + 2G*) × 100% and normalized against the WT level. The average of at least three independent measurements plus S.E. is shown. *C*, H2–2L and H2–3L were expressed in Sec61 WT and double mutant strains and analyzed as described in *A*. H2-segment membrane insertion (%) was calculated as 2G/(1G + 2G) × 100%. *D*, H2–5L was expressed in Sec61 WT and I83A/I91A double mutant cells. Cells were treated as in *A*, and membrane insertion of the H2-segment was calculated as in *B*.

H2-segment is not membrane-inserted, a single-glycosylated product results, whereas if it is membrane-inserted, a double-glycosylated form appears (Fig. 5*A*, *left panel*). For H2–2L, the major product was a single-glycosylated protein, and the minor product was a double-glycosylated protein, both of which became an unglycosylated protein upon endoglycosidase H treatment (Fig. 5*A*, *right panel*). Albeit little, a very faint cleaved product that migrated faster than the unglycosylated Lep-H2 was detected (Fig. 5*A*, *right panel*). Because the size of this band did not change upon endoglycosidase H treatment, it was unglycosylated. This cleaved unglycosylated protein only appeared when the H2-segment was not membrane-inserted. For H2–3L, the major product was double-glycosylated, and the minor product was single-glycosylated as judged by endoglycosidase H digestion (Fig. 5*A*, *right panel*). When the double-glycosylated product appeared, smaller size band was detected, and upon endoglycosidase H treatment the size was shifted down, indicating that it was glycosylated. It only appeared when the H2-segment was membrane-inserted, and it has been confirmed in Lundin *et al.* (27) that this cleavage occurs by the signal peptidase activity. We selected H2-segments with 2L/17A and 3L/16A, the H2-segment membrane insertion efficiency of which are ~20 and ~70%, respectively. The threshold hydrophobicity of the Lep-H1 (single-spanning) and Lep-H2 (double-spanning) model proteins was shown to be different (27), because the H1-segment must be inserted into the membrane alone, whereas H2-segment membrane insertion can be aided by the preceding TM segment (44); thus Lep-H1 requires higher hydrophobicity than the H2-segment in Lep-H2. For WT and all the mutant strains, the model protein was efficiently targeted, as little unglycosylated products were detected (Fig. 5*A*). For H2–2L and H2–3L, compared with the WT level, we observed two groups of mutations that either increased (V82A, I86A, S88A, and Q96A) or decreased (S83A, I91A, L95A, N290A, P292A, L295A, S301A, N302A, and Q308A) the membrane integration of the H2-segment (Fig. 5*B*). These gating mutant groups superimpose with those found with the Lep-H1 model protein with the exception of I293A, S301A, F304A, and Q308A. In the I293A and F304A Sec61 mutants, targeting and membrane insertion of the Lep-H1 protein were defective, but membrane insertion of the Lep-H2 protein was only mildly impaired (Figs. 2, *C* and *D*, and 5*B*). In the S301A and Q308A Sec61 mutants, membrane insertion of the H2–3L model protein was reduced by >30% compared with the WT (Fig. 5*B*),

whereas the targeting defect with the Lep-H1 model protein was moderate (Fig. 2*C*). We noticed that the targeting and membrane insertion of Lep-H1 was more severe in the TM2b mutants (S83A, M90A, I91A, Q93A, F94A, and L95A; 16–36% or an average of 23% reduced insertion relative to the WT) compared with the TM7 mutants (N290A, P292A, L295A, S301A, N302A, and Q308A; 7–22% or an average of 15% reduced insertion relative to the WT) (Fig. 2*C*). However, the membrane insertion of the H2-segment in H2–3L construct was more severely affected in the TM7 mutants (N290A, P292A, L295A, S301A, N302A, and Q308A; 26–46% or an average of 35% reduced insertion relative to the WT) than the TM2b mutants (S83A, M90A, I91A, Q93A, F94A, and L95A; 4–48% or an average of 16% reduced insertion relative to the WT) (Fig. 5*B*). These results may indicate that the initial binding of a signal anchor sequence may be mediated more by TM2b, whereas the membrane insertion of a succeeding TM segment is more influenced by TM7.

The Effects of Individual Mutations Are Additive—We tested whether a combination of individual mutations would have an additive effect on TM segment insertion. Sec61 double mutants with two Ala mutations that increased (V82A/I86A, V82A/Q96A, I86A/Q96A) or decreased (S83A/I91A) membrane insertion and mutants with both effects (V82A/I91A, S83A/Q96A, L295A/F304A) were prepared. The Lep-H2 model proteins (Fig. 5*A*) were expressed in these double mutants, and the membrane insertion efficiency of the H2-segment was assessed (Fig. 5*C*). The V82A/I86A, V82A/Q96A, and I86A/Q96A double mutants further enhanced the membrane insertion efficiency of the H2-segment compared with the respective single mutants, whereas S83A/I91A significantly decreased membrane insertion efficiency, indicating that the effect of Ala mutations in gating helices is cumulative. The combination of two Ala mutations that increased and decreased membrane insertion (V82A/I91A, S83A/Q96A, L295A/F304A) counterbalanced the opposing effects and showed membrane insertion levels between those of the individual mutants (Fig. 5*C*). In the I83A/I91A double mutant, the membrane insertion of H2–2L and H2–3L was significantly reduced, and the membrane insertion of the hydrophobic H2–5L ($\Delta G = -1.0$ kcal/mol), which was efficiently inserted in the WT (~96%), was also reduced to 58%, indicating that the lateral gate is either stabilized with the closed conformation or more difficult to open (Fig. 5*D*).

Bpa-induced Photocross-linking—To investigate which residues in TM2b and TM7 of Sec61 face one another to mediate the opening and closing of the gate, an *in vivo* photocross-linking approach was performed (40, 45). Each residue in TM2b (82–96) and TM7 (290–308) was systematically substituted with the amber codon (TAG), and tandem repeats of the Factor Xa protease site (5′-IEGRIEGR-3′) were introduced into the first (loop 1), second (loop 2), fifth (loop 5), sixth (loop 6), or seventh loop (loop 7) by site-directed mutagenesis (46, 47). We confirmed that the introduction of Factor Xa cleavage sites into the Sec61 loops did not disrupt the function of Sec61 by plasmid shuffling (Fig. 6*A*).

Our experimental procedures consisted of two steps: UV cross-linking and Factor Xa-mediated cleavage of Sec61. Bpa is a photoreactive unnatural amino acid and generates a cross-link to a molecule in close proximity under UV irradiation. Bpa was biosynthetically incorporated into the amber suppressor codon in Sec61. Whole cell lysates were subjected to UV irradiation at 365 nm for 30 min followed by IP and Factor Xa treatment and analyzed by SDS-PAGE and Western blotting.

The rationale behind this approach assumes that if TM2b and TM7 are cross-linked, the full-length product of Sec61 with a Factor Xa cleavage site in loop 6 (Sec61-Xa(loop 6)) will still be present after Factor Xa treatment (Fig. 6, *B* and *C*, *upper panels*). In contrast, without cross-linking, Sec61-Xa(loop 6) will be cleaved into two peptides (TM1–5 and TM6–10) (Fig. 6, *B* and *C*, *lower panels*). Because the triple HA tag for IP and Western blotting is located at the C terminus of Sec61, only the cleaved C-terminal portion of Sec61 will be detected.

Site-directed Photocross-linking Identified residues in TM2b and TM7 of Sec61 That Are in Close Proximity to One Another—All Bpa-incorporated Sec61 variants were subjected to UV irradiation and subsequent IP and Factor Xa treatment. By comparing the relative amounts of full-length Sec61 over the total product (full-length plus cleaved Sec61) in UV+/Factor Xa+ *versus* UV−/Factor Xa+, the efficiency of Sec61 intramolecular cross-linking was assessed. The efficiency of Factor Xa cleavage usually reached ~95%, and UV-activated cross-linking efficiency was maximal at 10–20%.

Sec61 variants with Bpa incorporated at residues Ile-86, Met-90, and Gln-93, with a Factor Xa site in loop 5, had ~10–20% cross-linking efficiency, indicating that these residues are cross-linked to a region between TM6 and TM10 of Sec61 (Fig. 7*A*). In the case of Ser-89, ~20% cross-linking efficiency was observed when the cleavage site was in loop 2, but no cross-linked products were detected when the cleavage site was in loop 5, indicating that Ser-89 is cross-linked to a region between TM3 and TM5.

To further narrow down the region where the Ile-86, Met-90, and Gln-93 residues were cross-linked, Factor Xa sites were engineered in loop 6. For Ile-86, the full-length product was dropped to <10%, whereas Met-90 and Gln-93 maintained ~10% of full-length products when loop 6 was cleaved (Fig. 7*A*). This result indicates that Met-90 and Gln-93 are cross-linked to a region between TM7 and TM10.

For Sec61 variants with Bpa incorporated in TM7 and a Factor Xa site located in loop 1 or loop 2, Met-294, Leu-295, and Ser-301 showed ~20% full-length products when the cleavage site was in loop 2, but the amount of full-length product was decreased for Leu-295 and Ser-301 when the cleavage site was in loop 1 (Fig. 7*A*). These data indicate that although Met-294 faces TM1 and TM2, Leu-295 and Ser-301 preferentially interact with TM2. Asn-302 showed ~10–15% cross-linking efficiency when the cleavage site was in loop 1, and Ile-303 showed ~15% cross-linking efficiency when the cleavage site was in loop 2, indicating that Asn-302 may weakly interact with TM1 and Ile-303 may interact with the TM2. Although Gln-93 showed ~10–15% cross-linking efficiency when the cleavage site was in loop 5 or loop 6, its cross-linking was abolished when the cleavage site was in loop 2. This contradictory result is puzzling but may indicate that local structural changes can affect cross-linking efficiency.

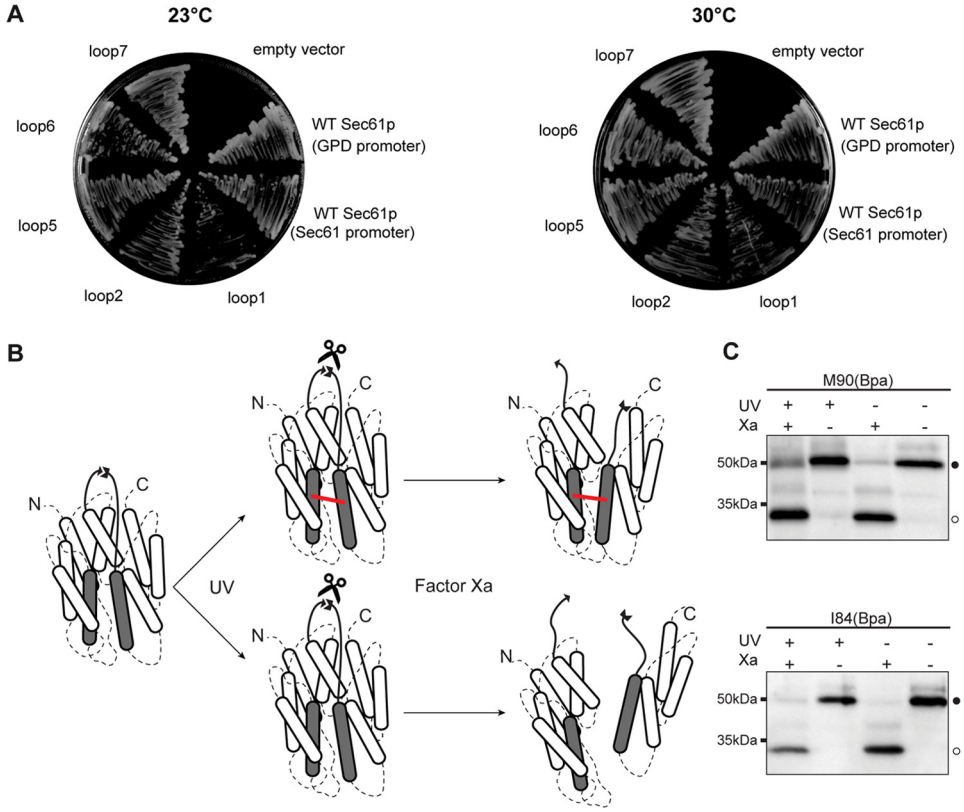

FIGURE 6. **Experimental scheme and Western blotting analysis of photocross-linking and Factor Xa cleavage.** *A*, yeast transformants with the indicated Factor Xa cleavage site insertion in Sec61 were grown on 5-fluoroorotic acid plates at 23 °C or 30 °C for 2 days. *B*, sequential experimental procedures are schematically drawn. The sixth loop with a Factor Xa cleavage site (loop 6) is indicated with a *solid line*. A *red line* represents cross-linking. *C*, samples were irradiated by UV as indicated, cleaved with Factor Xa, and subjected to SDS-PAGE and Western blotting. Full-length proteins and cleaved proteins are indicated as *closed* and *open circles*, respectively.

Overall, the cross-linking efficiency was low, which may reflect the flexible nature of gating helices because cross-linking would be more efficient if nearby residues were in constant contact rather than dynamically interacting. Thus, failure to cross-link does not mean that a residue is not in close proximity with other Sec61 TM segments. For the same reason, cross-linked residues may indicate that they are in close proximity and have a firm contact. The residues in TM2b that were cross-linked to TMs 7–10 or the residues in TM7 that were cross-linked to TM2b are the residues that showed a decrease in membrane insertion for model proteins when mutated to Ala (Met-90, Gln-93, Leu-295, and Ser-301). These results suggest that when the critical residues lining the interface of the lateral gate are mutated, two helices may collapse toward one another and stabilize the closed lateral gate; thus, these residues show relatively efficient cross-linking.

Our data are summarized in Fig. 7*B*. The corresponding homologous residues of cross-linked residues are indicated in blue. Ile-83 and Leu-261 in the *Methanocaldococcus jannaschii* SecY (Met-90 and Leu-295 in yeast, respectively) are located in closest proximity, facing each other. In the case of Gln-86 in SecY (Gln-93 in yeast), it is located near TM8 (Fig. 7*B*, *left* and *middle panels*). Moreover, the corresponding residues in *Thermotoga maritima*, Ile-90 and Ile-274 (Met-90 and Leu-295 in yeast), also face each other, even in the SecA-bound state (Fig. 7*B*, *right panel*). Finally, when we mapped Ser-281 in *T. maritima* (Ser-301 in yeast), it was located near the plug domain (colored in *orange*). These results indicate that the gating helices have high structural homology to the archaeal-bacterial TM2b and TM7 in terms of helix orientation and proximity of individual residues and thus suggest a high structural similarity between the eukaryotic Sec61 translocon and its archaeal-bacterial homolog SecY.

DISCUSSION

The structure of the archaeal and bacterial SecY translocon and earlier cross-linking studies indicated that TM2b and TM7 form the site where signal sequences bind and TM domains partition from the translocon channel into the lipid bilayer and has been referred to as the "lateral gate" (5–7) (9, 10). Guided by these earlier studies, we attempted to determine an interaction profile for the residues in the lateral gate of yeast Sec61 using an *in vivo* site-directed photocross-linking approach, and analyzed the effects of mutations of those residues using membrane insertion assays with a set of model proteins. Three main findings are summarized in the following.

First, data from cross-linking experiments show that Met-90 and Gln-93 in TM2b face TM7–10 and Leu-295 and Ser-301 in TM7 face TM2b. Corresponding residues in SecY structure show that they are in close proximity. When these residues were mutated to Ala one at a time, the membrane insertion efficiency of both single- and double-spanning membrane proteins was reduced. These results suggest that the mutation of the residues in the interface of the lateral gate may cause the

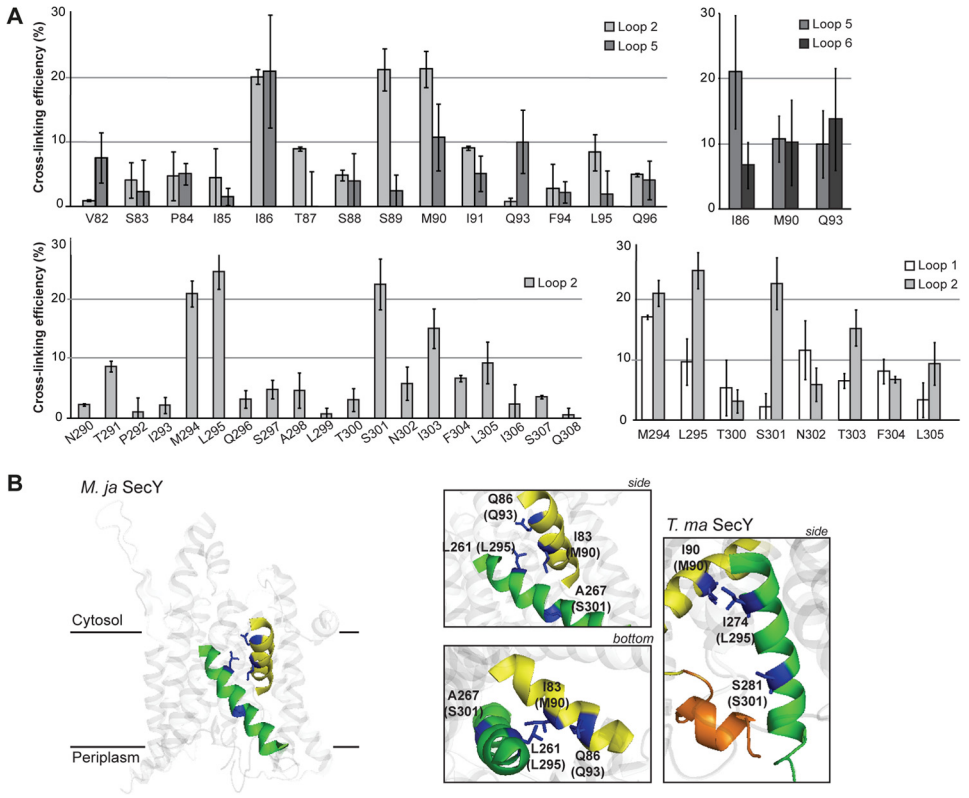

FIGURE 7. **Cross-linking efficiency of each residue in TM2b and TM7.** *A*, the cross-linking efficiency of each residue was calculated by comparing the amount of full-length UV+/Factor Xa+ *versus* UV−/Factor Xa+ proteins. Factor Xa cleavage sites were present in the indicated Sec61 loops. The average of at least three independent measurements plus S.D. is shown. *B*, corresponding residues of the cross-linked residues in yeast Sec61 are indicated in the SecY structure (*blue*) (PDB code 1RH5) (5), PDB code 3DIN) (13). The corresponding homologous residues in yeast are shown in *parentheses*. TM2b and TM7 are colored in *yellow* and *green*, respectively. TM2a (plug domain) is colored in *orange* (*right*). *M. ja*, *M. jannaschii*; *T. ma*, *T. maritima*.

collapse of the lateral gate and narrow the distance between two helices, hence making the gate harder to open. Thus, these residues may be the key residues guarding the lateral gate. It has been shown that disulfide bond formation between Ile-86/Phe-279 in *E. coli* SecY (Ile-86/Leu-295 in yeast Sec61) causes a translocation defect, suggesting that these residues are in close proximity and mediate the opening of the lateral gate (48).

Second, alanine scanning of Sec61 TM2b and TM7 identified mutants that increase the efficiencies of targeting and membrane insertion of model proteins. These residues are scattered across helices TM2b and TM7, and cross-linking data show that they face away from the lateral gate interface or are not cross-linked. We observed that these mutants allow membrane insertion to occur more quickly and facilitate membrane insertion of a single-spanning membrane protein in an N_{in}-C_{out} topology. These mutants exhibit similar phenotypes as *prl* mutants in *E. coli* (16–18), which allow the translocation of substrates carrying defective signal sequences. When Bondar *et al.* (23) examined the effect of *prl* mutations by molecular simulation, the interaction between the plug and pore region of SecY was loosened; thus the closed conformation was destabilized. They also suggested that when the closed conformation is destabilized, the channel pore allows more water molecules to enter (23). This polar environment of the channel pore may promote a single-spanning membrane protein to enter as a hairpin or insert into the ER membrane heads-in and then flip. Alternatively, the premature opening of the lateral gate may allow faster or increased contact with Sec62, which is located at the lateral exit site of Sec61. Recently, we have shown that Sec62 facilitates the membrane insertion of a TM segment in an N_{in}-C_{out} membrane topology (41). Therefore, faster or increased contact with Sec62 by the premature opening of the Sec61 lateral gate may enhance the membrane insertion of a TM domain in the N_{in}-C_{out} orientation.

Third, the degree of defects in targeting and membrane insertion differs depending on the type of a model protein between TM2b and TM7 Ala mutations. In the TM2b Sec61 variants M90A, Q93A, and F94A, the membrane insertion efficiency of a single-spanning membrane protein was reduced by ~20% compared with the WT. Interestingly, the membrane insertion of the second TM segment of a double-spanning membrane protein was only reduced by ~5%. In comparison, the TM7 Sec61 variants S301A, N302A, and Q308A showed a relatively greater defect in the membrane insertion of the downstream TM segment in a double-spanning membrane protein (H2–3L, reduced by ~35%) than a single-spanning membrane protein (Lep-H1(5L/14A), reduced by ~12%). These results may illustrate subtle differences in molecular mechanisms of signal sequence binding/initial opening of the lateral gate and membrane insertion of the downstream TM segment in multispanning membrane proteins that does not require initial opening of the channel.

An earlier photocross-linking study suggested that the hydrophobic core of a signal sequence (~12 residues) forms a

helical structure and binds between helices TM2 and TM7 as well as Sec62/71 (9). Twelve residues form an alpha helix with an estimated length of ~18 Å, which is roughly long enough to traverse the membrane half way. Based on these earlier studies and our present study, we speculate that the residues on the cytoplasmic side of TM2b may be critical for the recognition and binding of a signal (anchor) sequence and/or initiating the opening of the lateral gate, whereas TM7 has more influence on the membrane insertion of the succeeding TM segment in multispanning membrane proteins. Alternatively, our results may indicate that the first TM segment initiates opening of the lateral gate and remains near TM2b until the succeeding TM segment is translated and exits together through the lateral gate. If so, the succeeding TM segment would have less of an opportunity to interact with TM2b than TM7.

Acknowledgments—We thank Dr. Peter Schultz and Francis Peters (Scripps Research Institute) for providing reagents for BpA cross-linking studies and Dr. Martin Spiess (Biozentrum, Switzerland) for providing yeast strains.

REFERENCES

1. Zimmermann, R., Eyrisch, S., Ahmad, M., and Helms, V. (2011) Protein translocation across the ER membrane. *Biochim. Biophys. Acta* **1808,** 912–924
2. Rapoport, T. A. (2007) Protein translocation across the eukaryotic endoplasmic reticulum and bacterial plasma membranes. *Nature* **450,** 663–669
3. Deshaies, R. J., Sanders, S. L., Feldheim, D. A., and Schekman, R. (1991) Assembly of yeast Sec proteins involved in translocation into the endoplasmic reticulum into a membrane-bound multisubunit complex. *Nature* **349,** 806–808
4. Panzner, S., Dreier, L., Hartmann, E., Kostka, S., and Rapoport, T. A. (1995) Posttranslational protein transport in yeast reconstituted with a purified complex of Sec proteins and Kar2p. *Cell* **81,** 561–570
5. Van den Berg, B., Clemons, W. M., Jr., Collinson, I., Modis, Y., Hartmann, E., Harrison, S. C., and Rapoport, T. A. (2004) X-ray structure of a protein-conducting channel. *Nature* **427,** 36–44
6. Tsukazaki, T., Mori, H., Fukai, S., Ishitani, R., Mori, T., Dohmae, N., Perederina, A., Sugita, Y., Vassylyev, D. G., Ito, K., and Nureki, O. (2008) Conformational transition of Sec machinery inferred from bacterial SecYE structures. *Nature* **455,** 988–991
7. Egea, P. F., and Stroud, R. M. (2010) Lateral opening of a translocon upon entry of protein suggests the mechanism of insertion into membranes. *Proc. Natl. Acad. Sci. U.S.A.* **107,** 17182–17187
8. Park, E., and Rapoport, T. A. (2011) Preserving the membrane barrier for small molecules during bacterial protein translocation. *Nature* **473,** 239–242
9. Plath, K., Mothes, W., Wilkinson, B. M., Stirling, C. J., and Rapoport, T. A. (1998) Signal sequence recognition in posttranslational protein transport across the yeast ER membrane. *Cell* **94,** 795–807
10. Heinrich, S. U., Mothes, W., Brunner, J., and Rapoport, T. A. (2000) The Sec61p complex mediates the integration of a membrane protein by allowing lipid partitioning of the transmembrane domain. *Cell* **102,** 233–244
11. Demirci, E., Junne, T., Baday, S., Bernèche, S., and Spiess, M. (2013) Functional asymmetry within the Sec61p translocon. *Proc. Natl. Acad. Sci. U.S.A.* **110,** 18856–18861
12. Gogala, M., Becker, T., Beatrix, B., Armache, J. P., Barrio-Garcia, C., Berninghausen, O., and Beckmann, R. (2014) Structures of the Sec61 complex engaged in nascent peptide translocation or membrane insertion. *Nature* **506,** 107–110
13. Zimmer, J., Nam, Y., and Rapoport, T. A. (2008) Structure of a complex of the ATPase SecA and the protein-translocation channel. *Nature* **455,** 936–943
14. Junne, T., Schwede, T., Goder, V., and Spiess, M. (2007) Mutations in the Sec61p channel affecting signal sequence recognition and membrane protein topology. *J. Biol. Chem.* **282,** 33201–33209
15. Junne, T., Schwede, T., Goder, V., and Spiess, M. (2006) The plug domain of yeast Sec61p is important for efficient protein translocation, but is not essential for cell viability. *Mol. Biol. Cell* **17,** 4063–4068
16. Emr, S. D., Hanley-Way, S., and Silhavy, T. J. (1981) Suppressor mutations that restore export of a protein with a defective signal sequence. *Cell* **23,** 79–88
17. Li, W., Schulman, S., Boyd, D., Erlandson, K., Beckwith, J., and Rapoport, T. A. (2007) The plug domain of the SecY protein stabilizes the closed state of the translocation channel and maintains a membrane seal. *Mol. Cell* **26,** 511–521
18. Maillard, A. P., Lalani, S., Silva, F., Belin, D., and Duong, F. (2007) Deregulation of the SecYEG translocation channel upon removal of the plug domain. *J. Biol. Chem.* **282,** 1281–1287
19. Smith, M. A., Clemons, W. M., Jr., DeMars, C. J., and Flower, A. M. (2005) Modeling the effects of prl mutations on the *Escherichia coli* SecY complex. *J. Bacteriol.* **187,** 6454–6465
20. Trueman, S. F., Mandon, E. C., and Gilmore, R. (2011) Translocation channel gating kinetics balances protein translocation efficiency with signal sequence recognition fidelity. *Mol. Biol. Cell* **22,** 2983–2993
21. Junne, T., Kocik, L., and Spiess, M. (2010) The hydrophobic core of the Sec61 translocon defines the hydrophobicity threshold for membrane integration. *Mol. Biol. Cell* **21,** 1662–1670
22. Trueman, S. F., Mandon, E. C., and Gilmore, R. (2012) A gating motif in the translocation channel sets the hydrophobicity threshold for signal sequence function. *J. Cell Biol.* **199,** 907–918
23. Bondar, A. N., del Val, C., Freites, J. A., Tobias, D. J., and White, S. H. (2010) Dynamics of SecY translocons with translocation-defective mutations. *Structure* **18,** 847–857
24. Hessa, T., Kim, H., Bihlmaier, K., Lundin, C., Boekel, J., Andersson, H., Nilsson, I., White, S. H., and von Heijne, G. (2005) Recognition of transmembrane helices by the endoplasmic reticulum translocon. *Nature* **433,** 377–381
25. Hessa, T., Meindl-Beinker, N. M., Bernsel, A., Kim, H., Sato, Y., Lerch-Bader, M., Nilsson, I., White, S. H., and von Heijne, G. (2007) Molecular code for transmembrane-helix recognition by the Sec61 translocon. *Nature* **450,** 1026–1030
26. Hessa, T., Reithinger, J. H., von Heijne, G., and Kim, H. (2009) Analysis of transmembrane helix integration in the endoplasmic reticulum in *S. cerevisiae*. *J. Mol. Biol.* **386,** 1222–1228
27. Lundin, C., Kim, H., Nilsson, I., White, S. H., and von Heijne, G. (2008) Molecular code for protein insertion in the endoplasmic reticulum membrane is similar for N(in)-C(out) and N(out)-C(in) transmembrane helices. *Proc. Natl. Acad. Sci. U.S.A.* **105,** 15702–15707
28. Gumbart, J., Trabuco, L. G., Schreiner, E., Villa, E., and Schulten, K. (2009) Regulation of the protein-conducting channel by a bound ribosome. *Structure* **17,** 1453–1464
29. Ulmschneider, J. P., Smith, J. C., White, S. H., and Ulmschneider, M. B. (2011) In silico partitioning and transmembrane insertion of hydrophobic peptides under equilibrium conditions. *J. Am. Chem. Soc.* **133,** 15487–15495
30. Zhang, B., and Miller, T. F., 3rd. (2012) Long-timescale dynamics and regulation of Sec-facilitated protein translocation. *Cell Rep.* **2,** 927–937
31. Osborne, A. R., Rapoport, T. A., and van den Berg, B. (2005) Protein translocation by the Sec61/SecY channel. *Annu. Rev. Cell Dev. Biol.* **21,** 529–550
32. Ismail, N., Crawshaw, S. G., Cross, B. C., Haagsma, A. C., and High, S. (2008) Specific transmembrane segments are selectively delayed at the ER translocon during opsin biogenesis. *Biochem. J.* **411,** 495–506
33. Pitonzo, D., Yang, Z., Matsumura, Y., Johnson, A. E., and Skach, W. R. (2009) Sequence-specific retention and regulated integration of a nascent membrane protein by the endoplasmic reticulum Sec61 translocon. *Mol. Biol. Cell* **20,** 685–698
34. Hou, B., Lin, P. J., and Johnson, A. E. (2012) Membrane protein TM seg-

ments are retained at the translocon during integration until the nascent chain cues FRET-detected release into bulk lipid. *Mol. Cell* **48,** 398–408
35. Sadlish, H., Pitonzo, D., Johnson, A. E., and Skach, W. R. (2005) Sequential triage of transmembrane segments by Sec61α during biogenesis of a native multispanning membrane protein. *Nat. Struct. Mol. Biol.* **12,** 870–878
36. Cymer, F., and von Heijne, G. (2013) Cotranslational folding of membrane proteins probed by arrest-peptide-mediated force measurements. *Proc. Natl. Acad. Sci. U.S.A.* **110,** 14640–14645
37. Goder, V., Junne, T., and Spiess, M. (2004) Sec61p contributes to signal sequence orientation according to the positive-inside rule. *Mol. Biol. Cell* **15,** 1470–1478
38. Pilon, M., Schekman, R., and Römisch, K. (1997) Sec61p mediates export of a misfolded secretory protein from the endoplasmic reticulum to the cytosol for degradation. *EMBO J.* **16,** 4540–4548
39. Liu, C., Apodaca, J., Davis, L. E., and Rao, H. (2007) Proteasome inhibition in wild-type yeast *Saccharomyces cerevisiae* cells. *Biotechniques* **42,** 158, 160, 162
40. Chen, S., Schultz, P. G., and Brock, A. (2007) An improved system for the generation and analysis of mutant proteins containing unnatural amino acids in *Saccharomyces cerevisiae*. *J. Mol. Biol.* **371,** 112–122
41. Reithinger, J. H., Kim, J. E., and Kim, H. (2013) Sec62 Protein mediates membrane insertion and orientation of moderately hydrophobic signal anchor proteins in the endoplasmic reticulum (ER). *J. Biol. Chem.* **288,** 18058–18067
42. Wilkinson, B. M., Tyson, J. R., and Stirling, C. J. (2001) Ssh1p determines the translocation and dislocation capacities of the yeast endoplasmic reticulum. *Dev. Cell* **1,** 401–409
43. Finke, K., Plath, K., Panzner, S., Prehn, S., Rapoport, T. A., Hartmann, E., and Sommer, T. (1996) A second trimeric complex containing homologs of the Sec61p complex functions in protein transport across the ER membrane of *S. cerevisiae*. *EMBO J.* **15,** 1482–1494
44. Heinrich, S. U., and Rapoport, T. A. (2003) Cooperation of transmembrane segments during the integration of a double-spanning protein into the ER membrane. *EMBO J.* **22,** 3654–3663
45. Chin, J. W., Cropp, T. A., Anderson, J. C., Mukherji, M., Zhang, Z., and Schultz, P. G. (2003) An expanded eukaryotic genetic code. *Science* **301,** 964–967
46. Nelson, R. M., and Long, G. L. (1989) A general method of site-specific mutagenesis using a modification of the *Thermus aquaticus* polymerase chain reaction. *Anal. Biochem.* **180,** 147–151
47. Hemsley, A., Arnheim, N., Toney, M. D., Cortopassi, G., and Galas, D. J. (1989) A simple method for site-directed mutagenesis using the polymerase chain reaction. *Nucleic acids Res.* **17,** 6545–6551
48. du Plessis, D. J., Berrelkamp, G., Nouwen, N., and Driessen, A. J. (2009) The lateral gate of SecYEG opens during protein translocation. *J. Biol. Chem.* **284,** 15805–15814